Reduced phase error through optimized control of a superconducting qubit

Erik Lucero, ¹ Julian Kelly, ¹ Radoslaw C. Bialczak, ¹ Mike Lenander, ¹ Matteo Mariantoni, ¹ Matthew Neeley, ¹ A. D. O'Connell, ¹ Daniel Sank, ¹ H. Wang, ¹ Martin Weides, ¹ James Wenner, ¹ Tsuyoshi Yamamoto, ¹, ² A. N. Cleland, ¹ and John M. Martinis¹, *

¹Department of Physics, University of California at Santa Barbara, Broida Hall, Santa Barbara, CA 93106 ²Green Innovation Research Laboratories, NEC Corporation, Tsukuba, Ibaraki 305-8501, Japan (Dated: October 31, 2018)

Minimizing phase and other errors in experimental quantum gates allows higher fidelity quantum processing. To quantify and correct for phase errors in particular, we have developed a new experimental metrology — amplified phase error (APE) pulses — that amplifies and helps identify phase errors in general multi-level qubit architectures. In order to correct for both phase and amplitude errors specific to virtual transitions and leakage outside of the qubit manifold, we implement "half derivative" an experimental simplification of derivative reduction by adiabatic gate (DRAG) control theory. The phase errors are lowered by about a factor of five using this method to $\sim 1.6^\circ$ per gate, and can be tuned to zero. Leakage outside the qubit manifold, to the qubit $|2\rangle$ state, is also reduced to $\sim 10^{-4}$ for 20% faster gates.

Many candidate systems for quantum computation display several quantum energy levels, with computing architectures either employing just two of these levels [1– 12], or using three or more in ("d-level") qudit-based approaches [2, 6, 13]. Achieving good control over the computational states, while avoiding interference from the non-computational ones, requires measuring and understanding the source and magnitude of error-generating processes as well as correcting for such errors. For example, gate operations in the superconducting phase [2] and transmon [6] qubits, which are relatively weakly anharmonic, can generate leakage from the computational manifold to higher (non-computational) levels ("manifold leakage"). However, by careful experimental design one can identify and minimize the source of such errors, thereby improving qubit control.

Previous experiments identified the amplitude errors associated with manifold leakage by using error budgeting and metrology [14]. By directly measuring leakage using the Ramsey error filter protocol, this error is now understood and can be suppressed to $\sim 10^{-4}$ [14], at or near the threshold for fault-tolerant quantum computing [15, 16]. Randomized benchmarking, an alternative approach to measuring gate error, relies on a many-pulse protocol, effectively averaging over the Bloch sphere to quantify gate fidelity [16, 17]. Unfortunately, this approach optimizes a single value (gate fidelity) and does not distinguish between amplitude and phase errors. Quantum process tomography by contrast provides a complete analysis of gate operation [1, 18, 19], but requires calibrated $X_{\pi/2}$ and $Y_{\pi/2}$ pulses, which can themselves be error sources.

Phase errors also contribute to overall gate error, but the relative contribution differs from amplitude-related errors. Consequently, a method is needed to separately quantify the phase error generated by a gate. This will aid in identifying the source of these errors, improve calibration of high-fidelity tomography pulses, and provide a benchmark for optimizing control pulses.

In this Letter we explicitly show that gate errors can be separated into amplitude and phase errors. Virtual excitations to non-computational levels (e.g. the $|2\rangle$ state) during gate operation result in phase errors, while real excitations after the gate produce amplitude errors. In order to better quantify the phase errors, we introduce a new metrology, "amplified phase error" (APE) pulses, which uses a Ramsey fringe experiment to measure and amplify this ubiquitous source of error. We focus on errors related to $\pi/2$ pulses, because such pulses provide the basis for tomography and are essential in algorithms. We also demonstrate a simplified experimental version of the protocol [20] termed "derivative removal by adiabatic gates" (DRAG) [15], which we call "half-derivative" (HD) pulses. By using HD pulses together with APE metrology, we measure and reduce the phase error to 1.6° per gate, a factor of five reduction from unoptimized performance. As a demonstration of this method, we perform quantum state tomography to map out the trajectories of typical HD pulses, including a π -pulse and a rotation about an arbitrary axis, using X, Y and Z controls to implement an (off-equator) Hadamard gate. In addition, we show that APE metrology is a universal tool for probing phase errors on any of the higher qudit levels.

In the experiments described here, we used a single superconducting phase qubit with $T_1 = 450 \,\mathrm{ns}$ and $T_2^{\mathrm{echo}} = 390 \,\mathrm{ns}$. The circuit layout and operation have been described previously [2]. We have three-axis control over the qubit: microwave pulses of arbitrary amplitude and phase, resonant with the qubit $|1\rangle \leftrightarrow |0\rangle$ transition frequency f_{10} , produce rotations about any axis in the x-y plane, while current pulses on the qubit bias line adiabatically change the qubit frequency, causing phase accumulation between $|0\rangle$ and $|1\rangle$, generating z-axis rotations [21]. The $|2\rangle \leftrightarrow |1\rangle$ transition frequency f_{21} differs

 $^{{\}rm *Electronic~address:~martinis@physics.ucsb.edu}$

from f_{10} by $\Delta/2\pi = f_{21} - f_{10} \sim -200$ MHz (see Fig. 1a).

Non-ideal qubit behavior can arise from both leakage at the end of the gate and virtual transitions to higher states during on-resonant operations. The leakage is an amplitude error, representing loss of probability to states outside the manifold. Leakage can be reduced to $\sim 10^{-4}$ by careful shaping of the microwave envelope and choosing the correct gate duration, which scales as $1/\Delta$ [14, 22].

The phase error arising from virtual transitions (especially to the $|2\rangle$ state) can be modeled as effective qubit rotations about the z-axis. We first restrict ourselves to simple gates comprising π and $\pi/2$ rotations. An $X_{\pi/2}$ pulse (a rotation about the x-axis by an angle $\theta = \pi/2$) ideally produces the transformation

$$X_{\pi/2} = e^{-i\sigma_x \frac{\pi}{4}} = \frac{1}{\sqrt{2}} \begin{pmatrix} 1 & -i \\ -i & 1 \end{pmatrix} ,$$
 (1)

where σ_x is one of the Pauli matrices. From numerical simulations of our multi-level qubit, we find that this transformation, expressed in quantum circuit language, is instead

$$X'_{\pi/2} = e^{-i\epsilon'} Z_{\epsilon} X_{\pi/2} Z_{\epsilon} , \qquad (2)$$

where Z_{ϵ} is the phase error of interest and $0 < \epsilon \ll 1$ [23]. The leading term in Eq. (2) is a global phase and can be ignored. We note that Eq. (2) differs from $X_{\pi/2}^{\star} = Z_{-\epsilon}X_{\pi/2}Z_{\epsilon}$, which corresponds to a rotation about a new axis ϵ away from the x-axis in the x-y plane.

The phase error ϵ is a function of both the rotation angle θ and the gate time t_g . From simulations, we find that $\epsilon \sim \theta^2/t_g$. Longer gate times decrease the virtual transitions and consequently reduce the phase error, consistent with the AC-Stark effect [24].

In order to best reduce this error, we first sought a protocol that would amplify the error ϵ . If we consider a 2π rotation generated by concatenating four $\pi/2$ pulses, we find from Eq. (2) that $X_{\pi/2}^{\prime 4} = -e^{-4i\epsilon'}I$, where I is the identity [23]. A concatenated 2π rotation thus does not accumulate the relative phase error.

We next examine the pseudo-identity operation that is formed by concatenating positive and negative θ rotations. For a first-order expansion with $\epsilon \ll 1$ we find

$$I_{\theta}' = (Z_{\epsilon} X_{\theta} Z_{\epsilon}) (Z_{\epsilon} X_{-\theta} Z_{\epsilon})$$

$$\approx \begin{pmatrix} 1 + i(\cos \theta - 1)\epsilon & -(\sin \theta)\epsilon \\ (\sin \theta)\epsilon & 1 - i(\cos \theta + 3)\epsilon \end{pmatrix} , \quad (3)$$

where X_{θ} is an arbitrary rotation of θ about the x-axis [23]. For $\theta = \pi$ we find that $I'_{\pi} = e^{-2i\epsilon'}I$, which is similar to the 2π rotation, as the phase error ϵ cancels. However, for $\theta = \pi/2$ we find

$$I'_{\pi/2} = (Z_{\epsilon} X_{-\pi/2} Z_{\epsilon}) (Z_{\epsilon} X_{\pi/2} Z_{\epsilon})$$

$$\approx \begin{pmatrix} 1 - i\epsilon & \epsilon \\ -\epsilon & 1 - 3i\epsilon \end{pmatrix} , \tag{4}$$

showing phase error accumulation.

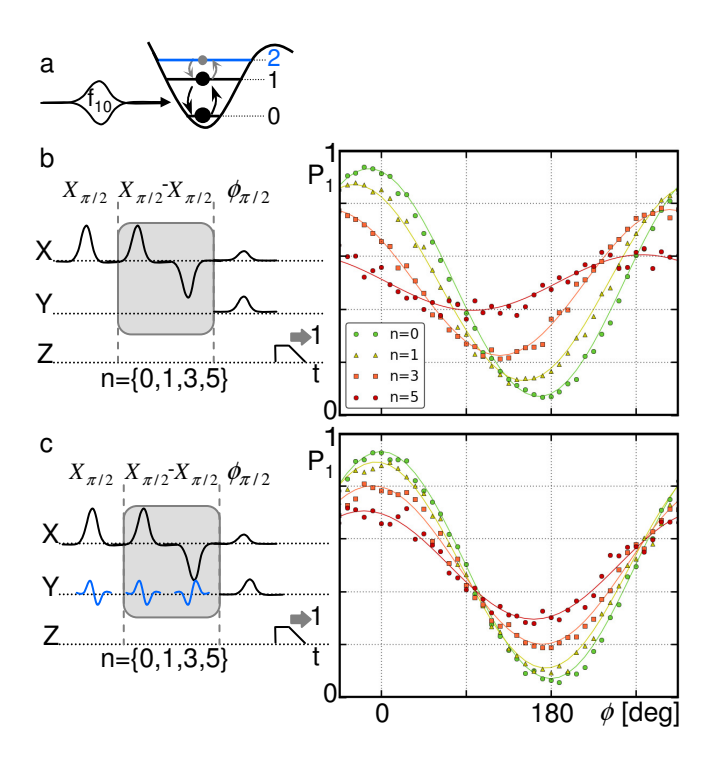


FIG. 1: (Color online) Multilevel qubit and amplified phase error (APE) metrology. (a) Qubit with three energy levels, illustrating phase error due to virtual transitions to the $|2\rangle$ state. While performing on-resonance $|0\rangle \leftrightarrow |1\rangle$ gate operations at frequency f_{10} , virtual transitions to $|2\rangle$ create a phase change in $|1\rangle$. (b) Left, single-control (X-quadrature) APE pulse sequence, where the pulse shape represents the microwave envelope. Ramsey-fringe experiments are modified by $I_{\pi/2}^{\prime n}$ $(n \in \{0,1,3,5\})$ pseudo-identity operations in-between the first $X_{\pi/2}$ and last $\phi_{\pi/2}$ pulses. At the end the Z control line is pulsed to measure the probability of $|1\rangle$. Right, the probability of measuring $|1\rangle$ as a function of the rotation axis ϕ of the final $\pi/2$ pulse. Fits to extract the phase shift are plotted as lines with the data (dots). (c) Left, same pulse sequence as in a, but with the addition of Y-quadrature "half-derivative" pulses, as discussed in the text. Right, the data (dots) with fits (lines) show small phase shifts for the HD pulse sequence.

To measure this error, we combine the result from Eq. (4) with a Ramsey fringe experiment, forming the "amplified phase error" (APE) sequence. The APE sequence consists of inserting n successive $I'_{\pi/2}$ pseudo-identity operations between the $\pi/2$ pulses that define a Ramsey fringe measurement (Fig. 1b). The phase error is amplified by 2n for n applications of the pseudo-identity operation,

$$I_{\pi/2}^{\prime n} \approx (Z_{2\epsilon})^n = Z_{2n\epsilon} \ . \tag{5}$$

By applying APE pulses to the state $|\psi\rangle = (|0\rangle - i|1\rangle)/\sqrt{2}$ followed by a final $\phi_{\pi/2}$ pulse, we directly probe the phase

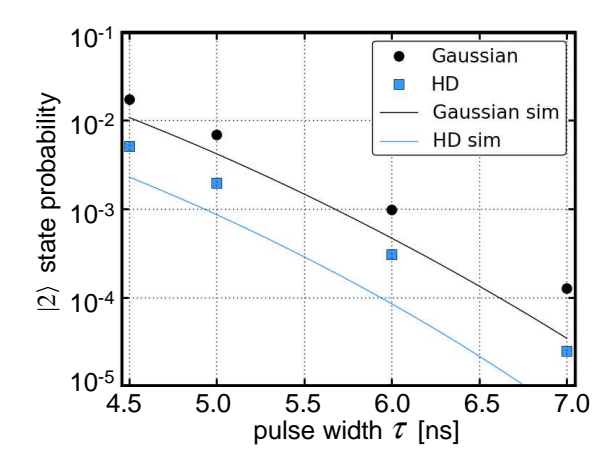


FIG. 2: (Color online) Amplitude errors due to leakage into the $|2\rangle$ state from an X_{π} -pulse. Plot of $|2\rangle$ error versus pulse width (FWHM) τ for single-control Gaussian (black dots) and HD (blue squares) π -pulses. The 6 ns HD pulse produces $\times 5$ lower error and 20% faster gates. The solid lines are three-state simulations using Gaussian (black) and HD (blue) pulses.

error due to the $X_{\pi/2}$ pulses.

Figure 1b shows the probability of measuring the $|1\rangle$ state versus rotation axis ϕ of the final $\phi_{\pi/2}$ pulse, for $I_{\pi/2}^{\prime n}$ (n=0,1,3,5) pseudo-identity operations. Consistent with Eq. (5), the phase error scales with n. For n=5 in Fig. 1b, the final pulse is $\sim 90^{\circ}$ out of phase, corresponding to a $10\times$ phase error amplification from a total of 11 pulses, yielding 7.3° phase error per gate. The oscillation amplitude is also reduced, due to decoherence.

To correct the phase error, we employ the derivative reduction by adiabatic gates (DRAG) protocol [15]. The original DRAG prescription uses three controls, X, Y, and Z. The X control provides the original envelopeshaping to the microwaves, which we implemented as a Gaussian in time with arbitrary amplitude A, $X = A \exp[-4\ln(2)(t-t_0)^2/\tau^2]$, where τ is the full-width-athalf-maximum (FWHM) and t_0 the time at the center of the pulse. The quadrature control $Y = -\dot{X}/\Delta$ is the time derivative of the X control scaled by the nonlinearity Δ . The Z control produces a dynamic detuning pulse during the gate that removes the effective z-rotations from the virtual transitions.

We find both in simulations and experiment that the Y and Z controls are not independent. For experimental simplicity, we set Z to zero and compensate by reducing the magnitude of the Y control by 1/2, to form the so-called "half-derivative" (HD) protocol [23]. For a Gaussian envelope on the X control, the HD pulses are as illustrated in Fig. 1c and differ from the DRAG pulses by the quadrature controls, $Y = -\dot{X}/(2\Delta)$, Z = 0. Experimentally, we found that HD performed as well as full DRAG.

The HD pulse sequence in Fig. 1c is the same as Fig. 1b,

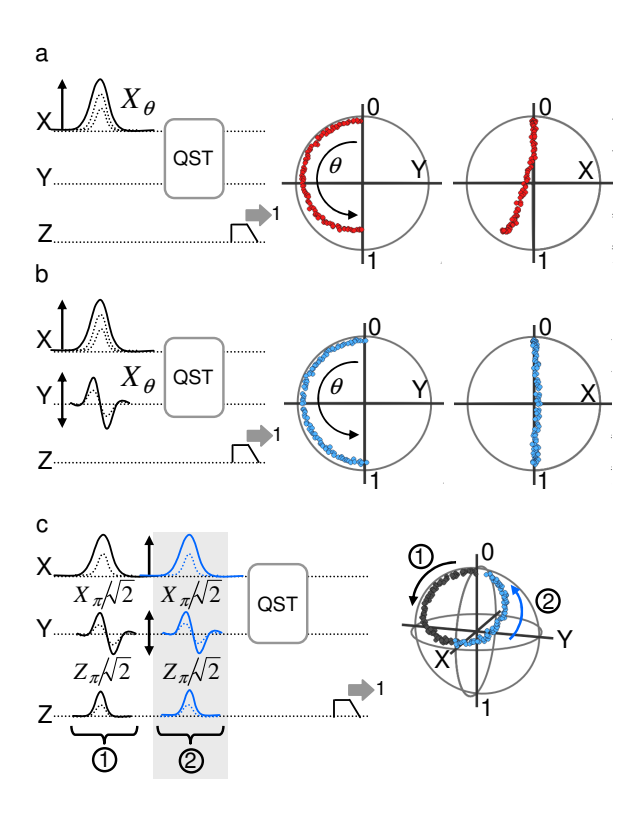


FIG. 3: (Color online) Gate trajectories using quantum state tomography (QST) for single control and HD pulses. (a) Left, pulse sequence for an X rotation. A Gaussian pulse of fixed length (FWHM = 6 ns) and varying amplitude completes the rotation angle to $\theta = \pi$. QST is performed at every incremental increase of amplitude. Right, the reconstructed quantum state data is plotted on the Bloch sphere from two perspectives, looking down the x and the -y axes. (b) Same as in a except using HD (X and Y simultaneous)control) pulses to perform the X rotation. No phase error is observed. (c) Left, pulse sequence of a two-part trajectory using HD pulses and Z control to form a Hadamard gate. X, Y, and Z controls are fixed-length (FWHM = $6 \, \mathrm{ns}$) pulses with increasing amplitudes to execute $\pi/\sqrt{2}$ rotations about X and Z. Trajectory 2 pulses ramp-up only after trajectory 1 pulses are at full amplitude. Right, the reconstructed QST data. Each trajectory completes a Hadamard gate, taking $|0\rangle \rightarrow (|0\rangle + |1\rangle)/\sqrt{2} \rightarrow |0\rangle.$

with the addition of the Y control. Data are plotted for the same number of $I'_{\pi/2}$ pseudo-identity operations. We find by applying the HD protocol the phase error is reduced to 1.6° per gate, and can be further minimized by tuning the amplitude of the derivative pulse.

HD pulses also reduce the leakage to the $|2\rangle$ state. Plotted in Fig. 2 are the data from a Ramsey error filter [14] for both single control Gaussian and HD pulses. A 6 ns (FWHM) HD X_{π} pulse gives a $|2\rangle$ state probability of 10^{-4} , almost an order of magnitude better than a non-HD pulse of the same width, which consequently provides a 20% faster gate [14].

With calibrated $X_{\pi/2}$ and $Y_{\pi/2}$ pulses, we can perform

quantum state tomography (QST) without worry of miscalibrated measurement axes. As a practical demonstration of how HD pulses reduce phase error, we perform QST [21] with and without HD. Figure 3a(b) shows the pulse sequence and data for the Gaussian pulses (HD pulses) during an X_{θ} rotation. The pulses are of fixed length (FWHM = 6 ns) with variable amplitude θ . QST is performed at each incremental increase of amplitude and the quantum state is recreated in the Bloch sphere as shown to the right of each of the respective pulse sequences. In contrast with the single control Gaussian pulses, the HD pulses execute a meridian trajectory with no phase error with increasing θ .

The final HD demonstration is an (off-equator) Hadamard gate, shown in Fig. 3c, which uses all three control lines [23]. We incrementally increase the amplitude of all three control lines using fixed length (FWHM = 6 ns) pulses to perform rotations from 0 to $\pi/\sqrt{2}$ about both the x and z axes, which at full amplitude gives the Hadamard gate H ($|0\rangle \rightarrow (|0\rangle + |1\rangle)/\sqrt{2}$). The trajectory concludes with a second set of pulses to complete the identity operation I = HH, and returning to the initial state $(|0\rangle + |1\rangle)/\sqrt{2} \rightarrow |0\rangle$.

We also consider the challenge of optimizing control pulses for each d-level of a qudit [2]. Tomography verifies the operation, but again relies on the calibrations of $\pi/2$ pulses. In principle, APE provides the necessary phase calibration certification for tomography.

To demonstrate the general utility of the APE protocol, we implement this metrology on the qudit level for state $|2\rangle$. We first calibrate the $(\pi)_{10}$ and $(\pi)_{21}$ pulses to generate the $|0\rangle \rightarrow |1\rangle$ and $|1\rangle \rightarrow |2\rangle$ transitions, respectively [2]. As shown in Fig. 4, we first prepare the $|1\rangle$ state via an HD π pulse so that we can then perform a Ramsey fringe experiment using the $|1\rangle$ and $|2\rangle$ states. The APE pulses are applied between the first and last $(\pi/2)_{21}$ pulses, only now resonant with f_{21} . The data are for single controlled Gaussian envelope pulses, i.e. no HD protocol for the $|1\rangle \rightarrow |2\rangle$ pulses.

Surprisingly, after n=5 pseudo-identity operations, only 12° of phase error is measured, equivalent to 1.1° per gate. We offer a qualitative interpretation: the relatively small anharmonicity of the phase qudit, combined with the symmetric virtual transitions to the $|3\rangle$ and $|0\rangle$ states, provide complementary phase shifts that partially cancel out the phase error.

In conclusion, we introduced a new metrology tool, amplified phase error (APE) pulses, which can amplify the phase error by an order of magnitude. Together with APE and half-derivative pulses, our simplified variant of DRAG [15], we identify and reduce phase errors to 1.6° per gate. By simply re-scaling the analytic form for the HD pulses, the phase error can be completely removed. The HD pulses also can increase gate speed by 20%.

We acknowledge discussions with Jerry Chow, Jay Gambetta, Felix Motzoi, and Frank Wilhelm. Devices were made at the UCSB Nanofabrication Facility, part of

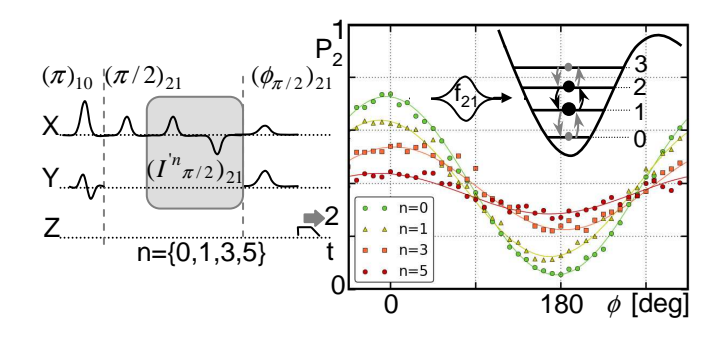


FIG. 4: (Color online) Multilevel qudit and APE metrology for the $|1\rangle\leftrightarrow|2\rangle$ transition. Inset, the four energy levels of the qudit illustrate the nearly symmetric virtual transitions to states $|3\rangle$ and $|0\rangle$ that mostly cancel the phase error during the f_{21} resonant drive. Left, pulse sequence showing $(\pi)_{10}$ for a $|0\rangle\to|1\rangle$ transition then a Ramsey fringe with the pseudoidentity operation on the $|1\rangle\leftrightarrow|2\rangle$ transition. Right, the probability of measuring the $|2\rangle$ state as a function of the rotation axis of the final $(\phi_{\pi/2})_{21}$ pulse for $n\in\{0,1,3,5\}$ pseudo-identity operations. With only a single control pulse (no HD correction), the phase error is 1.1° per gate.

the NSF-funded National Nanotechnology Infrastructure Network. M.M. acknowledges support from an Elings fellowship. This work was supported by IARPA under grant W911NF-04-1-02-4.

- M. A. Nielsen, I. L. Chuang Quantum Computation and Quantum Information (Cambridge Univ. Press, Cambridge 2000).
- [2] M. Neeley et al., Science **325**, 722 (2009).
- [3] J. I. Cirac and P. Zoller, Phys. Rev. Lett **74**, 4091 (1995).
- [4] N. A. Gershenfeld and I. L. Chuang, Science 275, 350 (1997).
- [5] R. Bianchetti et al., arXiv:1004.5504v1 (2010).
- [6] L.DiCarlo et al., Nature **460**, 240 (2009).
- [7] J. Q. You, F. Nori, Phys. Today 58, 42–47 (2005).
- [8] A. Imamoglu et al., Phys. Rev. Lett. 83, 4202 (1999)
- [9] J. R. Weber *et al.*, Proc. Natl. Acad. Sci. **107**, 8513 (2010)
- [10] P. M. Platzman and M. I. Dykman, Science 284, 1967 (1999)
- [11] J. R. Petta et al., Science **309**, 21802184 (2005)
- [12] J. M. Martinis et al., Phys. Rev. Lett. 89, 117901 (2002).
- [13] T. Yamamoto et al., arXiv:1006.5084v1.
- [14] E. Lucero et al., Phys. Rev. Lett. 100, 247001 (2008).
- [15] F. Motzoi, et al., Phys. Rev. Lett. 103, 110501 (2009).
- [16] E. Knill, Nature 434, 39-44 (2005).
- [17] J. M. Chow et al., Phys. Rev. Lett. 102, 090502 (2009).
- [18] M. Neeley et al., Nature Physics 4, 523 (2008).
- [19] R. C. Bialczak et al., Nature Physics 6, 409 (2010).
- [20] J. M. Chow et al., arXiv:100501v1.
- [21] M. Steffen et al., Phys. Rev. Lett. 97, 050502 (2006).
- [22] M. Steffen, J. M. Martinis, I. L. Chuang, Phys. Rev. B 68, 224518 (2003).
- [23] See supplemental material for more details.

[24] B. W. Shore Phys. Rev. A 17, 1739 (1978).

Supplemental: Reduced phase error through optimized control of a superconducting qubit

Erik Lucero, Julian Kelly, Radoslaw C. Bialczak, Mike Lenander, Matteo Mariantoni, Matthew Neeley, A. D. O'Connell, Daniel Sank, H. Wang, Martin Weides, James Wenner, Tsuyoshi Yamamoto, A. N. Cleland, and John M. Martinis^{1,*}

¹Department of Physics, University of California at Santa Barbara, Broida Hall, Santa Barbara, CA 93106

²Green Innovation Research Laboratories, NEC Corporation, Tsukuba, Ibaraki 305-8501, Japan

(Dated: October 31, 2018)

TRACKING QUBIT FREQUENCY

Optimized qubit control pulses rely on a precise measurement of the qubit transition frequency. After performing spectroscopy to find the qubit frequency f_{10} to within $\sim 1\,\mathrm{MHz}$, we fix the gate time τ and tune the microwave amplitude to execute a π rotation. We verify that the computed amplitude for $\pi/2$ rotation is indeed half that for a π rotation by performing two consecutive $\pi/2$ rotations and comparing the probability P_1 between that of a single π rotation.

Next, to precisely measure the qubit frequency, we use a Ramsey fringe experiment, where the final $\phi_{\pi/2}$ -pulse rotates at 50MHz about a variable axis on the equator of the Bloch sphere. A frequency shift in the oscillations of P_1 different from 50MHz is the amount the microwave drive is detuned from the qubit frequency. Correcting for this offset precisely tunes the microwave drive to the qubit frequency to within 1 part in 10^4 (sub MHz resolution), which is consistent with limits set from 1/f fluxnoise fluctuations[1].

We also can perform a more complete test (2-D scans) of this frequency calibration by noting that the phase error is $\epsilon = \delta f \delta t$ if the microwave drive is δf off-resonance from the qubit frequency for some time δt . Therefore, we verify that the microwave carrier matches the gubit frequency for the entire δt of the APE sequences via a Ramsey fringe experiment as shown in Fig. S1. Fig. S1b shows the data for two different detunings: left, $\delta f = 10 \,\mathrm{MHz}$ and right, $\delta f < 1\,\mathrm{MHz}$ (after performing the calibration described above). When the microwave drive is detuned by $\delta = 10 \,\mathrm{MHz}$ the data show a distinct tilt and clear oscillations with a frequency of 10 MHz. After calibration the data has no beating and therefore no sign of a detuned microwave drive. This confirms that the qubit frequency is tracked precisely throughout the duration of the desired (Amplified Phase Error) sequences.

To compute the nonlinearity $\Delta/2\pi = f_{21} - f_{10}$ for use in the HD protocol, we directly measure the transition frequency between states $|1\rangle$ and $|2\rangle$ with a Ramsey Error Filter (REF)[2]. The REF uses an oscillation, provides finer resolution, and is simpler to automate experimen-

FIG. S1. (Color online)Tracking the qubit frequency f_{10} . (a) Ramsey fringe sequence that consists of two Gaussian-shaped $\pi/2$ -pulses, separated in time by t, followed by a measure pulse on the Z-control tuned to tunnel the $|1\rangle$ state. The first $\pi/2$ -pulse defines the rotation axis; by convention this is the x-axis. The second pulse is delayed by a time t with variable rotation axis ϕ . (b) Plots of P_1 versus separation time t and phase ϕ for pulse sequence in **a**. Left, microwave drive is 10 MHz detuned from the qubit frequency f_{10} . Right, data taken after calibration; microwaves detuned less than 1 MHz from the qubit frequency.

tally than for peak-finding in high power spectroscopy. To increase the $|2\rangle$ state population, the $(\pi)_{10}$ pulses (for the $|0\rangle \leftrightarrow |1\rangle$ transitions) are sufficiently short and do not use the HD protocol. Using this technique, we measure the $|1\rangle \rightarrow |2\rangle$ transition frequency, f_{21} to within 1 MHz.

AMPLIFIED PHASE ERROR THEORY

From numerical simulations, an $X_{\pi/2}$ pulse has the transformation, (ignoring global phases), given by

$$X'_{\pi/2} \simeq Z_{\epsilon} X_{\pi/2} Z_{\epsilon} \,,$$
 (S1)

where Z_{ϵ} is the phase error of interest

$$Z_{\epsilon} = \begin{pmatrix} 1 & 0 \\ 0 & e^{-i\epsilon} \end{pmatrix} . \tag{S2}$$

a $X_{\pi/2}$ $\phi_{\pi/2}$ X
Y
Z

b
200 \overline{y} \overline{y}

^{*} martinis@physics.ucsb.edu

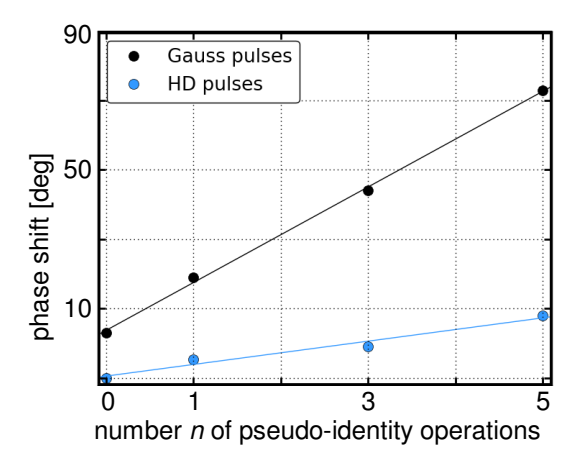


FIG. S2. Phase shift versus number n of pseudo-identity operations.

Using Eqs. (S1) and (S2), we explicitly calculate the phase shift for a 2π rotation coming from four $\pi/2$ pulses. For an arbitrary rotation θ about the x-axis, the gate operation is

$$X_{\theta} = \begin{pmatrix} \cos \theta/2 & -i \sin \theta/2 \\ -i \sin \theta/2 & \cos \theta/2 \end{pmatrix} , \qquad (S3)$$

such that $X'_{\pi/2}$ is

$$X'_{\pi/2} = \frac{1}{\sqrt{2}} \begin{pmatrix} 1 & -ie^{-i\epsilon} \\ -ie^{-i\epsilon} & e^{-i2\epsilon} \end{pmatrix} . \tag{S4}$$

(S5)

Concatenating four positive $\pi/2$ rotations results in

$$X_{\pi/2}^{\prime 4} \equiv (X_{\pi/2}^{\prime})^{4}$$

$$= \frac{1}{4} \begin{pmatrix} e^{-6i\epsilon} (-1 - e^{2i\epsilon} - 3e^{4i\epsilon} + e^{i\epsilon}) & -ie^{-7i\epsilon} (-1 + e^{2i\epsilon})^{2} (1 + e^{2i\epsilon}) \\ -ie^{-7i\epsilon} (-1 + e^{2i\epsilon})^{2} (1 + e^{2i\epsilon}) & e^{-8i\epsilon} (-1 + 3e^{2i\epsilon} + e^{4i\epsilon} + e^{6i\epsilon}) \end{pmatrix}$$

$$\simeq e^{-i4\epsilon} I, \tag{S6}$$

where I is the identity. Equation (S6) only acquires a global phase.

Next, we calculate the phase shift for the pseudo-identity operation, used in the APE protocol, comprised of a positive then a negative $\theta=\pi/2$ rotation.

$$I'_{\pi/2} = X'_{-\pi/2} X'_{\pi/2}$$

$$= \begin{pmatrix} e^{-i\epsilon} \cos(\epsilon) & e^{-2i\epsilon} \sin(\epsilon) \\ -e^{-2i\epsilon} \sin(\epsilon) & e^{-3i\epsilon} \cos(\epsilon) \end{pmatrix}$$

$$\approx \begin{pmatrix} 1 - i\epsilon & \epsilon \\ -\epsilon & 1 - 3i\epsilon \end{pmatrix}. \tag{S7}$$

For n applications of the pseudo-identity operation, in the limit where $0 < \epsilon \ll 1$, $\epsilon \to n\epsilon$

$$I_{\pi/2}^{\prime n} \approx \begin{pmatrix} 1 - in\epsilon & n\epsilon \\ -n\epsilon & 1 - 3in\epsilon \end{pmatrix}$$
, (S8)

and by removing an overall global phase

$$I_{\pi/2}^{\prime n} \approx (Z_{2\epsilon})^n = Z_{2n\epsilon} \,. \tag{S9}$$

The measured phase shift scales with the number n of pseudo-identity operations as shown in Fig. S2.

Z-PULSE CALIBRATION

Explicit Z gates are required for the (off-equator) Hadamard gate. We calibrate our Z pulse as shown in Fig. S3. A static length (full-width at half-max = 6ns)

with an increasing amplitude Z-pulse is inserted between two HD $\pi/2$ pulses with fixed separation time $t_{\rm fixed}$. The probability of measuring the $|1\rangle$ state P_1 oscillates with increasing $Z_{\rm amp}[3]$. The arrow indicates the $Z_{\rm amp}$ that corresponds to a rotation angle of π about the z-axis.

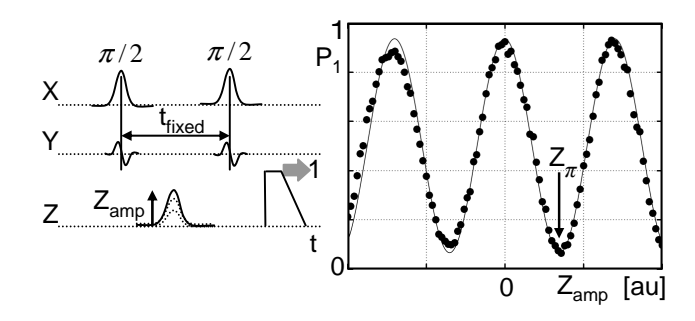


FIG. S3. Z_{π} calibration. (a) Left, the Ramsey-type pulse sequence to calibrate a Z_{π} with the X and Y controls using the HD protocol described in the manuscript. The sequence consists of two, 6ns (FWHM) $\pi/2$ - pulses fixed in time with $t_{\rm fixed}=24{\rm ns}$ and a 6ns (FWHM) Z-pulse centered in between them. The separation time is chosen to minimize overlap of the pulses. The $Z_{\rm amp}$ increases incrementally. Right, the probability of measuring the $|1\rangle$ state P_1 as a function of Z-pulse amplitude, $Z_{\rm amp}$. The data are plotted as points with best fit as a line. P_1 oscillates with increasing magnitude of the Z-pulse amplitude. Arrow indicates the Z-pulse amplitude equivalent to a π rotation about the Z-axis.

- [2] E. Lucero et~al., Phys. Rev Lett ${\bf 100},~247001~(2008).$ [3] M. Steffen et~al., Phys. Rev. Lett. ${\bf 97},~050502~(2006).$
- $[1]\ {\rm R.\ C.\ Bialczak}\ et\ al.,\ {\rm Phys.\ Rev\ Lett}\ {\bf 99},\ 187006\ (2007).$